Proceedings of ASME Turbo Expo 2021: Turbomachinery Technical Conference and Exposition
GT2021
June 7-11, 2021, Virtual Conference and Exhibition

GT2021-60347

ACCELERATED CREEP TEST (ACT) QUALIFICATION OF CREEP-RESISTANCE USING THE WCS CONSTITUTIVE MODEL AND STEPPED ISOSTRESS METHOD (SSM)

Jaime A. Cano[1] and Calvin M. Stewart[1]

Department of Mechanical Engineering
The University of Texas at El Paso
500 West University Avenue
Suite A126
El Paso, TX 79968-0521

ABSTRACT

In this study, a qualification of accelerated creep-resistance of Inconel 718 is assessed using the novel Wilshire-Cano-Stewart (WCS) model and the stepped isostress method (SSM) and predictions are made to conventional creep data. Conventional creep testing (CCT) is a long-term continuous process, in fact, the ASME B&PV III requires that 10,000+ hours of experiments must be conducted to each heat for materials employed in boilers and/or pressure vessel components. This process is costly and not feasible for rapid development of new materials. As an alternative, accelerated creep testing techniques have been developed to reduce the time needed to characterize the creep resistance of materials. Most techniques are based upon the time-temperature-stress superposition principle (TTSSP) that predicts minimum-creep-strain-rate (MCSR) and stress-rupture behaviors but lack the ability to predict creep deformation and consider deformation mechanisms that occur for experiments of longer duration. The stepped isostress method (SSM) has been developed which enables the prediction of creep deformation response as well as reduce the time needed for qualification of materials. The SSM approach has been successful for polymer, polymeric composites, and recently has been introduced for metals. In this study, the WCS constitutive model, calibrated to SSM test data, qualifies the creep resistance of Inconel 718 at 750°C and predictions are compared to CCT data. The WCS model has proven to make long-term predictions for stress-rupture, minimum-creep-strain-rate (MCSR), creep deformation, and damage in metallic materials. The SSM varies stress levels after time interval adding damage to the material, which can be tracked by the WCS model. The SSM data is calibrated into the model and the WCS model generates realistic predictions of stress-rupture, MSCR, damage, and creep deformation. The calibrated material constants are used to generate predictions of stress-rupture and are post-audit validated using the National Institute of Material Science (NIMS) database. Similarly, the MCSR predictions are compared from previous studies. Finally the creep deformation predictions are compared with real data and is determined that the results are well in between the expected boundaries. Material characterization and mechanical properties can be determined at a faster rate and with a more cost-effective method. This is beneficial for multiple applications such as in additive manufacturing, composites, spacecraft, and Industrial Gas Turbines (IGT).

Keywords: Creep-resistance, Inconel 718, Stepped Isostress Method (SSM), Accelerated Creep Testing (ACT), Wilshire Equations, WCS Model

NOMENCLATURE

ACT	Accelerated Creep Testing
CCT	Conventional Creep Testing
k_1	Wilshire rupture material constant (hr^{-u})
k_2	Wilshire MCSR material constant (hr^{v})
k_b	Boltzmann constant ($J \cdot K^{-1}$)
MCSR	Minimum-creep-strain-rate
NIMS	National Institute of Material Science
Q_c^*	Creep activation energy (kJ/mol)
R	Universal gas constant 8.314 (kJ/mol)
SIM	Stepped-Isothermal Method
SSM	Stepped-Isostress Method
T	Temperature ($^\circ C$)
T_0	Service temperature ($^\circ C$)

T_i	Stepped temperature ($^\circ C$)
TTP	Time temperature-precipitation diagram
TTSSP	Time-Temperature-Stress-Superposition Principle
TTT	Time-temperature diagram
$t_{0,i}$	Virtual start time (hr)
t_R	SSM rupture time (hr)
t_r	Rupture time (hr)
u	Wilshire rupture material constant (unitless)
V_ϕ^*	Activation volume for ϕ Eyring equation (cm^3)
V_λ^*	Activation volume for λ Eyring equation (cm^3)
v	Wilshire MCSR material constant (unitless)
$X_{\exp,i}$	Experimental data value
$X_{sim,i}$	Simulated data value
WCS	Wilshire-Cano-Stewart
$\dot{\varepsilon}_{cr}$	Creep strain rate (1/hr)
$\dot{\varepsilon}_{final}$	Final creep rate (1/hr)
$\dot{\varepsilon}_{\min}$	Minimum-creep-strain-rate (1/hr)
ϕ	Sinh damage rate material constant (unitless)
ϕ_0	Coefficient for ϕ Eyring equation (unitless)
ϕ_i	Shift factor
λ	Sinh creep strain rate material constant (unitless)
λ_0	Coefficient for λ Eyring equation (unitless)
σ_0	Service/Initial stress (MPa)
σ_c	Activation stress of the SSM (MPa)
σ_i	Stepped stress (MPa)
σ_{pr}	Projection stress (MPa)
σ_R	SSM rupture stress (MPa)
σ_{TS}	Ultimate tensile strength (MPa)
τ_0	Reference time (hr)
$\dot{\omega}$	Damage rate (1/hr)
ω	Damage (unitless)

1. INTRODUCTION

1.1. Motivation

Recent material developments have increased the need for material qualification in shorter periods of time. Turbomachinery and pressure vessel components are subject to high temperatures which promotes the need for new heat-resistance materials [1]. Materials are expected to be suitable for a 30-year service life for steam turbines, boiler components, and other high temperature applications such as Industrial Gas Turbines (IGT's) [2]. To qualify the creep-resistance of materials conventional creep tests (CCTs) are to be conducted. The ASME B&PV III code requires that newly developed materials must have 10,000+ hours of experiments for each heat to be approved for service [3]. As material development has increase, particularly with newly additive manufacturing technologies, this process has become too costly and not feasible; especially, considering the uncertainty of creep testing. It has been shown for multiple steels that uncertainty governs data, where, if the same conditions of temperature and stress are given, a scatter on creep curves is projected [4]. Conversely, attempts to lessen the uncertainty with different combinations of temperature and stress results in a similar scatter [5]. As a result of, cost, uncertainty, protocols for testing; newly discovered materials are put into service in a period of 10-20 years. Material designs and processes must be accelerated to provide faster solutions to problems like efficiencies for turbomachinery, steam turbines, and other energy-based applications [6]. There is a need for accelerated testing methods that can characterize materials faster and models that can predict creep behaviors reliably. In this study, the creep-resistance of material Inconel 718 is assessed using an accelerated creep test (ACT) method called the stepped-isostress method (SSM) and the novel WCS model.

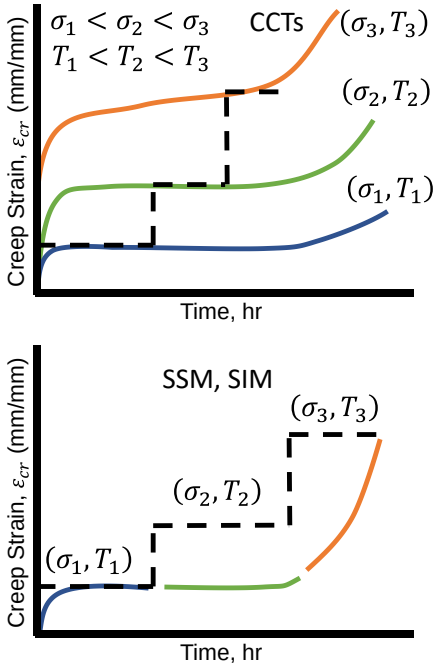

Figure 1: Time-temperature-stress superposition principle (TTSSP) illustrated with conventional creep test (CCTs) and then projected in the accelerated creep test (ACT) for either stepped-isostress method or stepped-isothermal method (SIM). Note that the dotted line is the stepped increase of either stress or temperature.

1.2. Stepped-Isostress Method (SSM)

Accelerated methods such as ACT are well-accepted to determine the remaining life of components at elevated temperatures [7]. These ACT methods have been established using conditions such as a linear cumulative damage law, stress

ratio cyclic loading for fatigue applications, and the time-temperature-stress superposition (TTSSP) principle [7-8].

It has been proven experimentally, that stress has a similar impact as temperature in viscoplastic materials [9]. This suggests that stress, temperature, and time can be manipulated to decrease the duration of experiments, as it describes the accelerated aging process [10]. The TTSSP in creep deformation can be used if the creep-strain-rate of an experiment conducted at elevated temperatures or stress can replicate that of a CCT as shown in Figure 1. Although both temperature and stress variations can be performed together, this method is typically divided into two types, the stepped-isothermal method (SIM) and the stepped-isostress method (SSM). Typically this relationship is given in the following form

Conventional **SIM** **SSM**

$$\dot{\varepsilon}_{cr}(\sigma_0, T_0, t) = \dot{\varepsilon}_{cr}\left(\sigma_0, T_i, \frac{t-t_{0,i}}{\phi_i}\right) = \dot{\varepsilon}_{cr}\left(\sigma_i, T_0, \frac{t-t_{0,i}}{\phi_i}\right) \quad (1)$$

where $\dot{\varepsilon}_{cr}$ is creep strain rate, T_0 is the service temperature, σ_0 service stress, T_i, and σ_i are the stepped temperature and stress, ϕ_i the shift factor, and $t_{0,i}$ is the virtual start time. Multiple stepped increases can be performed to a specimen and ϕ_i is calculated using empirical equations.

In this study, SSM is used as a preferred method, as it is easier experimentally to obtained load control rather than temperature control. Using the empirical equations, the SSM method has been assess for multiple polymers and polymeric composite materials and has been successful [11-18]. Recently, the SSM has been exploited to be used in metals as well. In a study conducted by Stewart et. al, a SSM test matrix captured the observed creep-resistance phenomenon with the hyperbolic sine model, or Sinh [19]. In doing so, this study provided strong evidence that the SSM approach could be extended to metallic materials. There still work to be done, as the CCTs were used during the calibration process. The Sinh model has some limitations as some constants have stress and temperature dependency, alternative models, such as the WCS, can be utilized to verify how well SSM performs with metallic materials.

1.3. Problem Statement

Past work has shown a variety of applications of the SSM in polymer and polymeric composite materials. However, SSMs require further development for applications with metal alloys [19-20]. The Sinh model has some limitations as most material constants are obtained purely numerically. Some other material constants have stress and temperature dependency. There have not been extrapolative and interpolative predictions using solely the SSM data for metallic materials, which would not only prove the feasibility of the method but would allow turbomachinery industries to perform short time SSM experiments and make CCT predictions even when data is not given.

2. RESEARCH OBJECTIVES

The objective of this study is to qualify the accelerated creep-resistance of Inconel 718 using the novel WCS model and SSMs to predict CCTs. Data is provided from previous studies of Inconel 718 at 750°C [19]. The SSM data of this study is used to calibrate the model. After calibrating the SSMs, and with the obtained material constants, the results are compared to Inconel 718 data obtained from studies conducted by the National Institute of Material Science (NIMS), Asadi, as well as the CCTs obtained from Stewart et al [19,21-23].

3. MATERIALS AND TEST METHODS

3.1. Inconel-718

Inconel-718 is a nickel-based superalloy used in elevated temperature applications due to its heat and corrosion resistance. Applications of nickel-based superalloys are on aviation, combustion systems, gas turbines and others as it is creep resistant as well [24]. The unique properties of nickel-based alloys such as Inconel 718 are attributed to the strengthening phases γ′-Ni3(Al, Ti) and γ"-Ni3Nb precipitates [24-25].

Specimen used in the study conducted by Stewart is heat treated to $1325\,^{\circ}F$ for 8 hours, furnace cooled at $100\,^{\circ}F/hr$ to $1150\,^{\circ}F$ and held for 8.25 hours, and air cooled for a total aging time of 18 hours [19]. The chemical composition as reported from the mill test report (MTR) is shown in Table 1.

Table 1: Chemical composition (wt%) of IN718

Element	MTR	Element	MTR
Ni	52.55	C	0.04
Cr	18.52	Mn	0.05
Fe	18.2	Si	0.08
Nb	5.2	P	0.007
Mo	2.92	S	0.0005
Ti	0.93	B	0.004
Al	0.52	Cu	0.05
Co	0.52		

The average ultimate tensile strength of the specimen presented from Stewart as well as the ones reported by the NIMS database are shown in Table 2. It is observed that the ultimate tensile strength (UTS) of Stewart's specimens is lower, this is due to the larger and coarser grains obtained from the slow cooling rate [19]. Although, the coarse grains lead to a higher creep resistance. This study considered the NIMS and Asadi's data sets to post-audit validate the predictions made from the calibrated SSM data. The stress-rupture data from NIMS are presented for five isotherms (550, 600, 650, 700, 750 °C) at multiple heat treatments with their respective UTS. The study from Asadi has MCSR data for three isotherms (593, 649, 704 °C) but no UTS is reported, therefore, the average from NIMS is used for predictions.

Table 2: Average ultimate tensile strength IN718

Source	Temperature (°C)	UTS (MPa)
Stewart's	750	689
NIMS	550	1224
NIMS	593	1218
NIMS	600	1217
NIMS	649	1145
NIMS	650	1144
NIMS	700	1003
NIMS	704	988
NIMS	750	818

Additionally, the creep activation energy, Q_c^* of Inconel 718 has been determined by Sellers model to be between 300-450 kJ/mol. Other studies from Shöcks-Seeger-Wolf and by Chaturvedi reports values between 175-225 or 264 kJ/mol [26-27]. Although Q_c^* can be determined analytically, it has been discussed by Cedro that using the value obtained by literature is accurate enough for many applications [28]. As discussed for the ultimate tensile strength, the coarser gains give lower mechanical properties to the specimen, making it unrealistic to assume the higher properties suggested by Seller. Therefore in this study, Q_c^* is assumed to be 200 kJ/mol which is the midpoint of the range suggested by Shöcks-Seeger-Wolf and Chaturvedi.

3.2. SSM Test

Table 3: SSM and CCT data for IN718 at 750°C [19].

Specimen ID	Initial Stress σ_0	MCSR at σ_0	Rupture Time t_r	Creep Ductility at t_r
	(MPa)	($hr^{-1}\times10^{-6}$)	(hr)	(%)
SSM_100	100	4.00	85.95	13.8
SSM_150	150	2.86	68.42	11.7
SSM_200	200	7.98	61.25	14.7
SSM_250	250	18.8	62.88	13.3
SSM_300	300	155	52.37	14.6
CCT_100	100	8.17	1535.4	2.85
CCT_200	200	50.0	362.5	27.7
CCT_300	300	155	89.1	15.5
CCT_350	300	376	42.72	13.1

The test matrix proposed by Stewart's study is to perform CCTs at 750 °C at multiple stress level (100, 200, 300, and 350 MPa). The data is used for post-audit validation as those CCTs are not included in the calibration method. Five SSMs are performed as well at 750 °C with different initial stresses (100, 150, 200, 250, and 300 MPa) and a final stress of 350 MPa. Four steps are considered, and the step size is defined as (final stress – initial stress)/(N-1) where N is the number of steps. The SSM considers deformation mechanism maps and hold times of 5 hours using time-temperature (TTT) and -precipitation (TTP) diagrams. The resulting creep behavior is shown in Table 3 [19].

4. CALIBRATION METHOD

4.1. WCS Model

Recently, a new model has been developed for creep deformation, damage, and rupture time predictions called the WCS model [29]. The WCS model consist of two coupled differential equations for creep-strain-rate and damage evolution as follows

$$\dot{\varepsilon}_{cr} = \frac{\left[-\ln\left(\frac{\sigma}{\sigma_{TS}}\right)\Big/ k_2\right]^{\frac{1}{v}}}{\exp\left(Q_c^*/RT\right)}\exp\left(\lambda\omega\right) \tag{2}$$

$$\dot{\omega} = \frac{\left[1-\exp(-\phi)\right]}{\phi}\frac{\exp\left(-\frac{Q_c^*}{RT}\right)}{\left[-\ln\left(\frac{\sigma}{\sigma_{TS}}\right)\Big/ k_1\right]^{\frac{1}{u}}}\exp\left(\phi\omega\right) \tag{3}$$

where σ_{TS} is the ultimate tensile strength, Q_c^* the creep activation energy, R is the universal gas constant, T is temperature, k_1, u, k_2, v are Wilshire material constants and λ, ϕ are Sinh material constants.

The WCS model combines the best features of the continuum damage mechanics (CDM) framework of the Sinh model and the Wilshire model. The Wilshire model consist of two equation of the following form

$$\frac{\sigma}{\sigma_{TS}} = \exp\left(-k_1\left[t_f\exp\left(-\frac{Q_c^*}{RT}\right)\right]^u\right) \tag{4}$$

$$\frac{\sigma}{\sigma_{TS}} = \exp\left(-k_2\left[\dot{\varepsilon}_{\min}\exp\left(\frac{Q_c^*}{RT}\right)\right]^v\right) \tag{5}$$

where $\dot{\varepsilon}_{\min}$ is the MCSR and both k_1 and u are obtained by plotting $\ln\left[-\ln\left(\sigma/\sigma_{TS}\right)\right]$ versus $\ln\left[t_f\exp\left(-Q_c^*/RT\right)\right]$ where the slope is u and k_1 is the y-intercept. Similarly, by plotting $\ln\left[-\ln\left(\sigma/\sigma_{TS}\right)\right]$ versus $\ln\left[\dot{\varepsilon}_{\min}\exp\left(Q_c^*/RT\right)\right]$ k_2 and v are

obtained. The remaining constants λ and ϕ come from the Sinh model were, to obtain λ, the following form is considered

$$\lambda = \ln\left(\dot{\varepsilon}_{final} / \dot{\varepsilon}_{\min}\right) \tag{6}$$

where $\dot{\varepsilon}_{final}$ is the final creep rate. Material constant λ is unique for every combination of stress and temperature and controls the creep curve trajectory. Although it can be obtained through an analytical approach, there is no limitation to use numerical methods. The remaining constant ϕ can be obtained both analytically and numerically, as well. In this study, ϕ and λ are obtained numerically using the following objective function

$$\sqrt{\frac{1}{N}\sum_{i=1}^{N}\left(\log\left(X_{\exp,i}\right)-\log\left(X_{sim,i}\right)\right)^2} \tag{7}$$

where $X_{\exp,i}$ and $X_{sim,i}$ are the experimental and simulated data values respectively and N is the number of data points. After both λ and ϕ constants are calibrated, an Eyring equation is employed to address the stress and temperature dependency of the constants. The Eyring equation is in the following form

$$\lambda = \lambda_0 \exp\left(\frac{V_\lambda^* \sigma}{k_b T}\right) \tag{8}$$

$$\phi = \phi_0 \exp\left(\frac{V_\phi^* \sigma}{k_b T}\right) + 1 \tag{9}$$

where V_λ^* and V_ϕ^* are activation volumes, k_b is the Boltzmann constant, λ_0, and ϕ_0 are material constants.

Overall the WCS model has been successful fitting long-term data of alloy P91 and has an explicit stress and temperature dependency [29]. However, the model has not been exploited in accelerated methods before. There are additional considerations that must be considered to apply the SSM data.

4.2. Modified SSM Method

While the WCS model has a clear calibration approach, there exist some limitations and considerations to the method when applying it to SSM. In conventional test methods, rupture time is a physically meaningful property as it relates to the actual critical point of the material. In SSM, due to the increments of stress and the damage caused by the multiple steps, rupture at the final stress does not necessarily correlates to the actual material rupture time. This does not allow the conventional WCS and Wilshire methods to calibrate both k_1 and u as it depends on the actual rupture times. Similarly, to calibrate λ, the final rate must be considered which, at the final stress step on the SSM, is also affected by the additional damage caused by the stress increase. However, the MCSR can be considered as a conventional value, as it reaches in the first step, before any damage is added through the stress stepping. Hence, k_2 and v can be calculated using the conventional Wilshire approach.

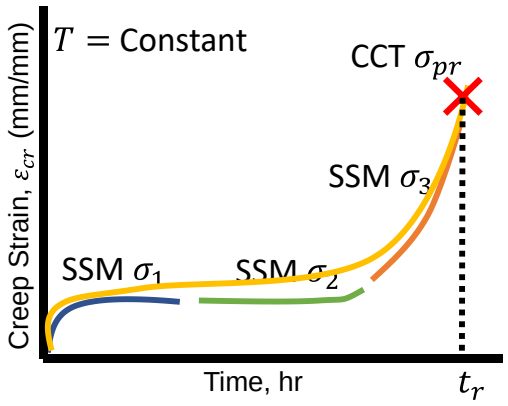

Figure 2: Stress projection of a CCT imitating the rupture path of an SSM curve with multiple steps. Note: the projection stress does not simulate the entire SSM curve.

Although these limitations exist, each SSM has a particular path that is like that of a CCT. In fact, each SSM has a similar rupture to a corresponding CCT with a corresponding stress as shown in Figure 2. A stress is projected and mimics the conditions at the last step. The stress projected, σ_{pr}, therefore, corresponds to an actual rupture time. The projection stress does not attempt to simulate all the SSM, only the last step.

To project this stress a relationship between stress and rupture is considered from the study conducted by Tanks [17]. Tanks considers an energy-based failure criterion and in this study the equation is modified in the following form

$$\sigma_{pr} = \frac{\sigma_R^2}{\sqrt{\left(\frac{2\sigma_c}{\sigma_0}\right)\left(\frac{t_R}{\tau_0}\right)^n + 1}} \tag{10}$$

where σ_R and t_R are the stress and rupture time of the SSM experiment, σ_c is an activation stress, τ_0 is a reference time, and n is a fitting constant. Note that on the study conducted by Tanks $\sigma_c = D$ and $\sigma_0 = C_0$. The model was modified from those unitless constants and applied real values to project the stress. The reference time considered in this study is the stepping time use in the SSM which is 5 hours. Material constants σ_c and n are fitting values estimated to be 4 MPa and 0.5, respectively. After [Eq. (10)] is applied, the projected stresses are obtained and shown in Table 4. Notice that for SSM_100 the projected stress and rupture time is like the one reported in CCT 300 as shown in Table 3. It was expected that if at 300 MPa the rupture time is 89.1 then the projected stress for a rupture of 85.96 should be slightly greater. Therefore, this method is close to actual CCTs as hypothesized. Considering that the projected stresses are related to the rupture times, the Wilshire method for calibrating k_1 and u can be followed as well as the given method to calibrate λ.

Table 4: Projected stress using [Eq. (*10*)]

Specimen ID	Initial Stress	Rupture Time	Projection Stress
SSM_100	100	85.95	303.31
SSM_150	150	68.42	316.74
SSM_200	200	61.25	324.16
SSM_250	250	62.88	328.87
SSM_300	300	52.37	332.12

5. RESULTS AND DISCUSSION

5.1. Wilshire Material Constants

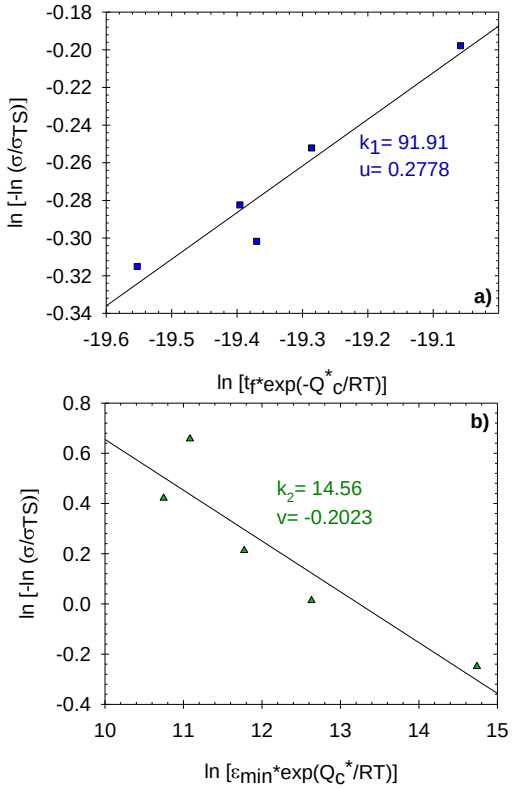

Figure 3 a): Material constants for stress-rupture k_1 and u and **Figure 3 b):** Material constants for minimum-creep-strain-rate (MCSR) k_2 and v obtained.

Considering that $Q_c^* = 200\ kJ/mol$, the plots to calibrate k_1, u, k_2, and v are shown in Figure 3 a) and b). Using the data gather from the SSM experiments at the first step as shown in Table 3 k_2 and v are obtained. There is one discrepancy where in SSM_300 does not reach the MCSR. Therefore, only for that case the second step is considered which is at 316 MPa. To calibrate k_1 and u the stress used is the obtained projection stress from Table 4. With the obtained results predictions for both stress-rupture and MCSR can be made from [Eq. (4)] and [Eq. (5)]. A summary of such material constants is shown in Table 5.

Table 5: Summary of Wilshire material constants for [Eq. (4)] and [Eq. (5)]

Q_c^*	k_1	u	k_2	v
kJ/mol	hr^{-u}	unitless	hr^{v}	unitless
200	91.91	0.2778	14.56	-0.2023

5.2. Stress-Rupture and MCSR Predictions

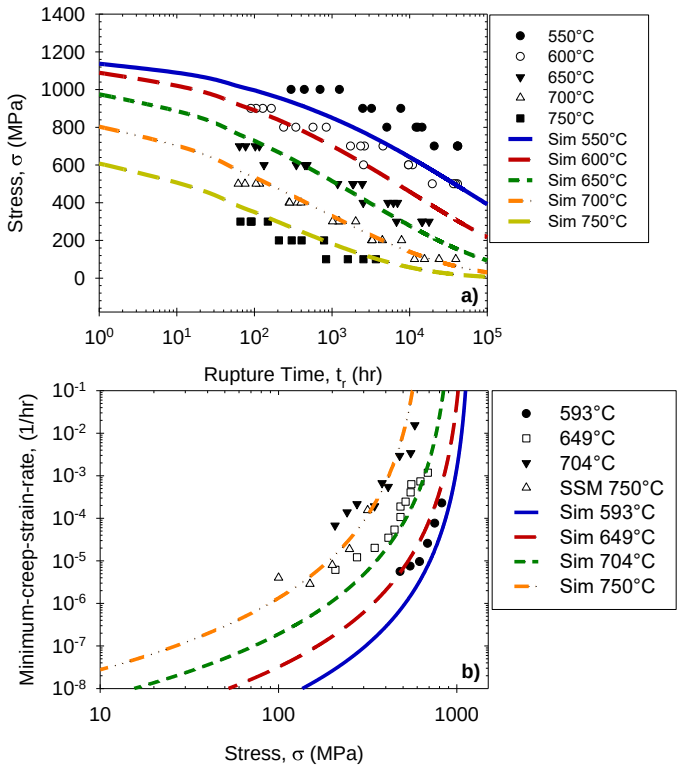

Figure 4 a): Stress-rupture prediction from [Eq. (4)] and **Figure 4 b):** Minimum-creep-strain-rate from [Eq. (5)]. Data for a) is from NIMS and for b) is from Asadi

Once the material constant k_1, u, k_2, and v are obtained predictions for both stress rupture and MCSR are attained as shown in Figure 4 a) and b). These predictions did not use any of the data sets from their respective sources. Rather, the material constants are shown in Table 5, obtained from the SSM experiments. Quantified error is provided in Table 6 for both stress rupture and MCSR prediction using the objective function given in [Eq. (7)].

The post-audit validated stress-rupture predictions from Figure 4 a) are made using the NIMS database. The NIMS database contains multiple heat treatments and the actual UTS

use for each prediction are the average as shown in Table 2. It is shown that predictions are consistent and sit well between the expected uncertainty band. Predictions are made for multiple heat treatments and isotherms using accelerated data. In Table 6 it is shown that most of the errors are < 0.5 which is typically an acceptable value for root error logarithmic functions (RMSE, RMLSE, etc.) although this can vary for different studies. The Sim 550 $^{\circ}C$ is the only one that exceeds this parameter. This is expected as the farthest the extrapolative is from the temperature used in calibration (750 $^{\circ}C$) the less accurate the results would be. Such trend is consistent for every other isotherm.

The MCSR predictions have more uncertainty as shown in Figure 4 b). The data used was obtained from Asadi and the UTS is the same as the one for NIMS, shown in Table 2. In this plot, the MCSR data obtained from the SSM experiments is plotted as well and it is shown to have a similar rate to that of temperature 704 $^{\circ}C$. Comparing the rates of SSM 750 $^{\circ}C$ and Asadi's 704 $^{\circ}C$, shows that the SSM material has a greater creep resistance. The trend expected for a material performing at higher temperatures is typically of a higher rate. This adds uncertainty to the model, as the predictions are capturing the performance of a material with a greater creep resistance. Therefore, predictions are not consistent to that data set and a probabilistic study is needed to reveal the reliability bands to analyze how well between the bands the predictions are. In fact, in Table 6 it is shown that every error exceeds 0.5. Regardless, the trend is consistent and is safe to hypothesized that if the materials were of the same quality, even with the SSM method, it would extrapolate with accuracy. Predictions for both stress-rupture and MCSR are consistent, validating the feasibility of the SSM experiments.

Table 6: Stress rupture and MCSR prediction errors using objective function [Eq. (7)]

Stress rupture	Error	MCSR	Error
Sim 550 $^{\circ}C$	0.82	Sim 593 $^{\circ}C$	0.67
Sim 600 $^{\circ}C$	0.44	Sim 649 $^{\circ}C$	1.40
Sim 650 $^{\circ}C$	0.25	Sim 704 $^{\circ}C$	1.63
Sim 700 $^{\circ}C$	0.19		
Sim 750 $^{\circ}C$	0.38		

5.3. Lambda and Phi Calibration

After predictions for stress-rupture and MCSR are made the remaining material constants to predict creep deformation and damage are λ and ϕ. In this study, both λ and ϕ are obtained numerically using [Eq. (7)] as the objective function. The error is minimized, and the resulting material constants are given in Table 7. Notice there is a significant discrepancy on SSM_250 as it is experimentally proven to not be consistent with the remaining experiments. The remaining error is shown for the entire creep curve.

Table 7: Summary of λ and ϕ with the error.

Specimen ID	λ	ϕ
SSM_100	5.18	1.7898
SSM_150	4.95	1.6450
SSM_200	5.25	1.8456
SSM_250	3.94	2.3452
SSM_300	5.45	1.7514

The calibrated material constants obtained from Table 7 are used to calibrate Eyring's [Eq. (8)] and [Eq. (9)] as well as he projection stresses from Table 4. Material constants are shown in Table 8 obtained through numerical optimization.

Table 8: Eyring's material constants [Eq. (*8*)] and [Eq. (*9*)]

λ_0	V_λ^*	ϕ_0	V_ϕ^*
Unitless	cm^3	Unitless	cm^3
2.89	2.60E-23	0.026	1.54E-22

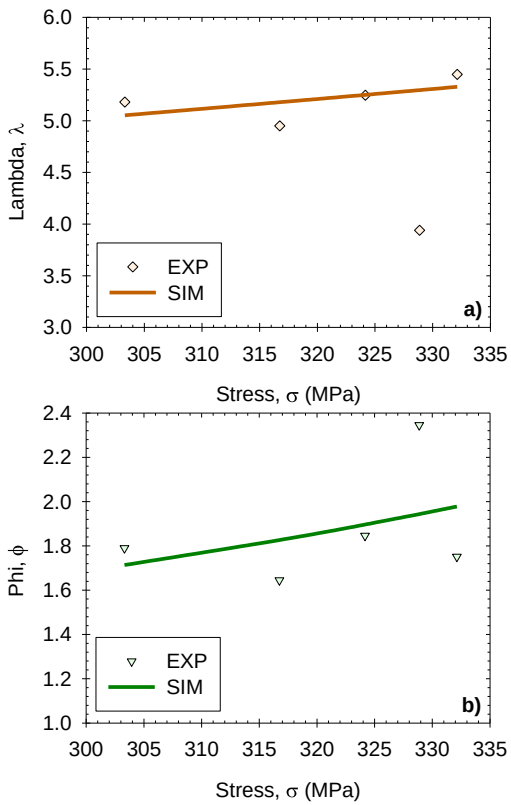

Figure 5 a): Predictions for lambda, λ using [Eq. (8)] and **Figure 5 b):** Predictions for phi, ϕ using [Eq. (9)].

The Eyring model is plotted to predict both λ and ϕ at multiple stress levels and isotherms if necessary. The plots for these material constants are given in Figure 5.

5.4. Creep Deformation and Damage Predictions

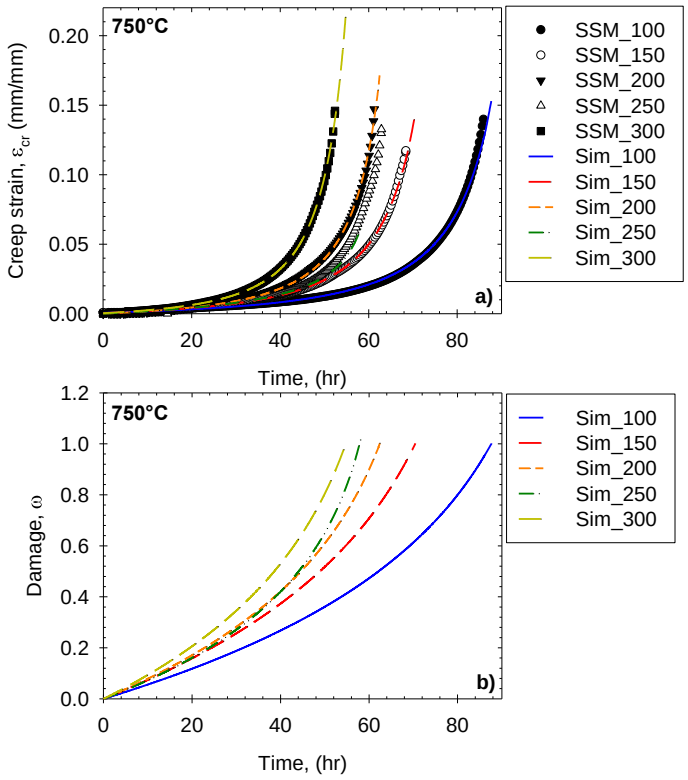

Figure 6 a): Creep deformation SSM fitting for [Eq. (2)] and **Figure 6 b):** Damage predictions using [Eq. (3)].

Using the Wilshire material constants obtained shown in Table 5 and the Sinh material constants shown in Table 7 the SSM data is fitted. The SSM data fits are shown in Figure 6 for both a) creep deformation and b) damage using [Eq. (2)] and [Eq. (3)]. A summary of the error of SSM and the CCT predictions are given in Table 9.

Table 9: Error summary for the SSM fitting and the CCT predictions using [Eq. (7)].

SSM	Error	CCT	Error
SSM_100	0.0660	CCT_100	0.6229
SSM_150	0.0395	CCT_200	0.7847
SSM_200	0.1082	CCT_300	0.0891
SSM_250	0.1299	CCT_350	0.1608
SSM_300	0.0138		

It is shown that the model fits the data accurately with a minor overestimation of ductility. In SSM_250, the model reaches failure, damage equal to unity, too fast not allowing a proper ductility estimation. This is due to the uncertainty of this data set. It is expected that SSM_250 sits between SSM_300 and SSM_200 but instead crosses SSM_200. In fact, it has a higher rupture time than SSM_200 which is unrealistic. The model is analytical in nature and the fitting numerical constants, λ and ϕ, do not capture such behavior. Regardless, the error is in a considerable error range as shown in Table 9. From there the model is accurate and consistent fitting the SSM data.

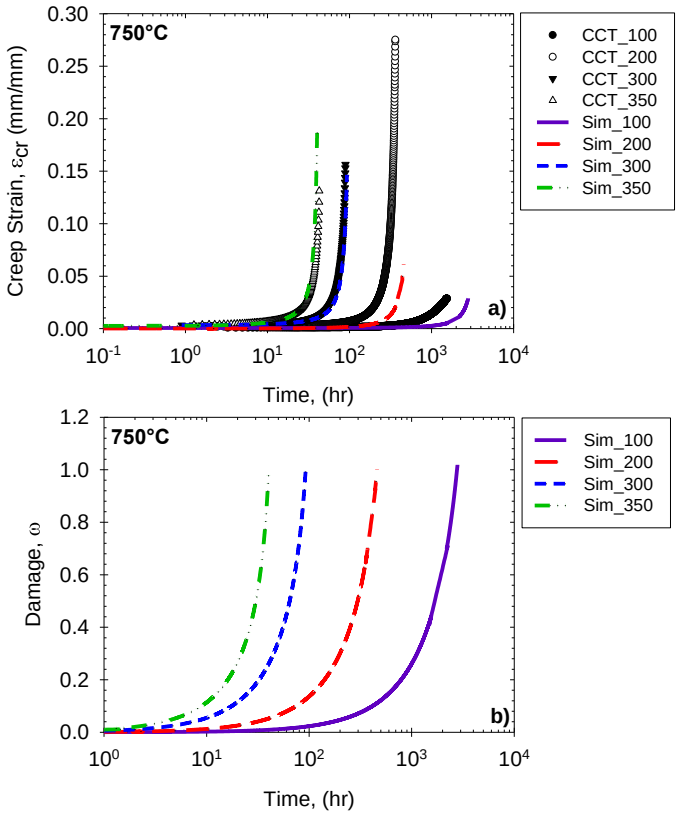

Figure 7 a): Creep deformation predictions using [Eq. (2)] and **Figure 7 b):** Damage predictions using [Eq. (3)] both for CCT data.

Using both the material constants obtained from Table 5 and the Eyring model shown in Figure 5 predictions for CCT are made. The predictions are shown in Figure 7 a) and b) for creep deformation and damage, respectively. In Table 9 it is shown that CCT_100 and CCT_200 exceed 0.5. This does not necessarily suggest the model fails as it can be determined qualitatively that the MCSR and rupture times are accurate. In fact, the only non-accurate rupture prediction is CCT_100, which is expected, as it has the longest rupture time (+1500 hours) and is predicted with less than 90 hours of experiments. Rather, most of the error is cause by the ductility. The data itself shows discrepancy in ductility as it is not consistent with the expected creep trend. Creep ductility increased from CCT_350 to CCT_300 and then

to CCT_200. Typically, the lower the stress, the less creep ductility is reported. The model attempts to capture this behavior and it is shown as the error decreases from CCT_200 to CCT_100 which would not be expected to. It is important to considered that the CCT predictions are made blindly as none of the data is used in the calibration process. This validates more the predicting capabilities that can be obtained using both the SSM and WCS model. Using the predictions, the creep resistance of Inconel 718 has been verified as, using this method, multiple parametric studies can be performed to predict the expected creep behavior.

6. CONCLUSIONS AND FUTURE WORK

In conclusion, the objective of qualifying the accelerated creep-resistance of Inconel 718 using the novel WCS model and SSM and predict CCTs has been achieved. This combined methodology has shown the ability to predict stress-rupture for multiple heats and isotherms and MCSR predictions. The model has shown the ability to fit the SSMs properly and can extrapolate and predict CCT.

Future work would be to consider some of the unrealistic features of the data, as shown in the SSM_250, to obtained more accurate results. Extending the work of this study would be to considered multiple calibration methods for different applications. Future work is to exploit this method and compared the resulting calibration and the error. Future work is to exploit these methods and compare them o this study and provide error and probabilistic analysis.

REFERENCES

[1] Takasawa, K., and Miki, K., 2018, "Development of High- and Intermediate-Pressure Steam Turbine Rotors for Efficient Fossil Power Generation Technology," The Japan Steel Works LTD Technical Review, No. 20.

[2] Robert Purgert, Jeffrey Phillips, Howard Hendrix, John Shingledecker, and James Tanzosh, 2016 "Materials for Advanced Ultrasupercritical Steam Turbines - Advanced Ultra-supercritical Component Demonstration," US Department of Energy, Technical Report, DOI: 10.2172/1332274

[3] ASME, 2015, ASME Boiler and Pressure Vessel Code, Section III, Division 1, Subsection NH – Class 1, Components in Elevated Temperature Service, New York, NY.

[4] Hossain, M. A., Cano, J. A., & Stewart, C. M. (2020, August). Probabilistic Creep Modeling of 304 Stainless Steel Using a Modified Wilshire Creep-Damage Model. In Pressure Vessels and Piping Conference (Vol. 83860, p. V006T06A040). American Society of Mechanical Engineers.

[5] Verma, A. K., Hawk, J. A., Romanov, V., & Carter, J. L. (2020). Predictions of long-term creep life for the family of 9–12 wt% Cr martensitic steels. Journal of Alloys and Compounds, 815, 152417.

[6] National Science and Technology Council, "Advanced Manufacturing: A Snapshot of Priority Technology Areas Across the Federal Government," Office of Science and Technology Policy, Washington, DC, 2016.

[7] Viswanathan, R., and Foulds, J., 1998, "Accelerated Stress Rupture Testing for Creep Life Prediction – Its Value and Limitations," Journal of Pressure Vessel Technology, 120(2), pp. 105-115.

[8] Nakada, M. (2019). Accelerated testing methodology for long-term creep and fatigue strengths of polymer composites. In Creep and Fatigue in Polymer Matrix Composites (pp. 325-348). Woodhead Publishing.

[9] Luo, W., Wang, C., Hu, X., & Yang, T. (2012). Long-term creep assessment of viscoelastic polymer by time-temperature-stress superposition. Acta Mechanica Solida Sinica, 25(6), 571-578.

[10] Peng, Q., Zhu, Z., Jiang, C., & Jiang, H. (2019). Effect of stress relaxation on accelerated physical aging of hydrogenated nitrile butadiene rubber using time-temperature-strain superposition principle. Advanced Industrial and Engineering Polymer Research, 2(2), 61-68.

[11] Jazouli, S., Luo, W., Bremand, F., and Vu-Khanh, T., 2005, "Application of time–stress equivalence to nonlinear creep of polycarbonate," Polymer testing, 24(4), pp. 463-467.

[12] Luo, W. B., Yang, T. Q., and An, Q. (2001). Time-temperature-stress equivalence and its application to nonlinear viscoelastic materials. Acta Mechanica Solida Sinica, `(3), 195-199.

[13] Luo, W. B., Wang, C. H., and Zhao, R. G., 2007, "Application of time-temperature-stress superposition principle to nonlinear creep of poly (methyl methacrylate)," Key Engineering Materials, 340, pp. 1091-1096.

[14] Giannopoulos, I.P. and Burgoyne, C.J., 2011, "Prediction of the long-term behavior of high modulus fibers using SSM," Journal of Materials Science, 46(24), pp. 7660-7671.

[15] Giannopoulos, I. P., and Burgoyne, C. J., 2012, "Accelerated and real-time creep and creep-rupture results for aramid fibers," Journal of Applied Polymer Science, 125(5), pp. 3856-3870.

[16] Tanks, J.D., Rader, K., and Sharp, S.R., 2015, "Accelerated creep testing of CFRP with the stepped isostress method," Mechanics of Composite and Multi-functional Materials, 7(46), Springer International Publishing, Editor K. Zimmerman.

[17] Tanks, J., Rader, K., Sharp, S., & Sakai, T. (2017). Accelerated creep and creep-rupture testing of transverse unidirectional carbon/epoxy lamina based on the stepped isostress method. Composite Structures, 159, 455-462.

[18] Hadid, M., Guerira, B., Bahri, M., & Zouani, A. (2014). Assessment of the stepped isostress method in the prediction of long-term creep of thermoplastics. Polymer testing, 34, 113-119.

[19] Stewart, C. M., Hossain, Md.A., Mach, R., Pellicote, J., Alexander, D. & Siddiqui, S.F. (2020). Accelerated Creep Testing of Inconel 718 using the Stepped Isostress Method (SSM). Material Performance and Characterization, ASTM.

[20] Mach, R., Pellicotte, J., Haynes, A., & Stewart, C. (2019, June). Assessment of Long Term Creep Using Strain Rate Matching From the Stepped Isostress Method. In Turbo Expo: Power for Land, Sea, and Air (Vol. 58684, p. V07AT31A011). American Society of Mechanical Engineers.

[21] NIMS, 2011, NIMS Creep Data Sheet No.59 - Data sheets on the elevated-temperature properties of Nickel Based 19Cr-18Fe-3Mo-5Nb-Ti-Al Corrosion-Resisting and Heat-Resisting Superalloy Bars (JIS NCF 718-B), National Institute for Materials Science, Japan

[22] C. G. McKamey, E. P. George, C. T. Liu, J. A. Horton, C. A. Carmichael, R. L. Kennedy,W. D. Cao, "Manufacturing on Nickel-Base Superalloys with Improved High Temperature Performance", Oak Ridge National Laboratory, Lockheed Martin, 2000.

[23] Asadi, M., Guillot, D., Weck, A., Hegde, S. R., Koul, A. K., Sawatzky, T., & Saari, H. (2012, July). Constructing a validated deformation mechanisms map using low temperature creep strain accommodation processes for nickel-base alloy 718. In ASME 2012 Pressure Vessels and Piping Conference (pp. 65-73). American Society of Mechanical Engineers.

[24] Zhang, H., Zhang, K., Lu, Z., Zhao, C., & Yang, X. (2014). Hot deformation behavior and processing map of a γ′-hardened nickel-based superalloy. Materials Science and Engineering: A, 604, 1-8.
[25] Ni, T., & Dong, J. (2017). Creep behaviors and mechanisms of Inconel718 and Allvac718plus. Materials Science and Engineering: A, 700, 406-415.
[26] Gujrati, R., Gupta, C., Jha, J. S., Mishra, S., & Alankar, A. (2019). Understanding activation energy of dynamic recrystallization in Inconel 718. Materials Science and Engineering: A, 744, 638-651.
[27] Chaturvedi, M. C., & Han, Y. (1989). Creep deformation of Alloy 718. Institute of Aeronautical Materials.
[28] Cedro, V., Garcia, C., & Render, M. (2018). Use of the Wilshire Equations to Correlate and Extrapolate Creep Data of HR6W and Sanicro 25. Materials, 11(9), 1585.
[29] Cano, J. A., & Stewart, C. M. (2021). A continuum damage mechanics (CDM) based Wilshire model for creep deformation, damage, and rupture prediction. Materials Science and Engineering: A, 799, 140231.